

Load-Displacement Characteristics and Interactive Load Capacity Model for Metal Plate Connections in Wood(Ⅱ)*1

– Interactive Load Capacity Model and Experimental Verification –

Moon-Jae Park*2 · Hee-Suk Jung*3

木材-金屬플레이트 接合部の 荷重-變位 特性 및 組合荷重性能에 대한 模型 分析 (Ⅱ)*1

– 組合荷重模型과 實驗的 立證 –

朴 文 在*2 · 鄭 希 錫*3

要 約

高度의 엔지니어링 構造物로 경제성이 높은 輕量 木造트러스에 사용될 수 있는 소나무(*Pinus densiflora*) 材에 적용한 20게이지 아연도금 鋼 플레이트 接合部の 組合荷重 및 모멘트 性能을 평가하기 위하여 정밀도를 改善한 偏心加力 裝置를 裝置하여 實驗하고 半剛節 接合부의 概念과 假想 方法을 적용한 模型을 유도하여 非線形 解析하였다.

半剛節 接合부의 概念을 도입하여 저자가 유도한 非線形 模型으로 조합하중 하에서의 接합부 거동을 해석한 결과, 금속 플레이트 接합부의 모멘트는 Wolfe 模型에 비하여 精確도가 높은 값으로 計算되었는데, 이는 비선형模型에서 接합부의 半剛性에 의한 2차적인 모멘트의 影響을 적절히 고려한 때문으로 판단되었다. 본 연구에서 사용한 實驗장치는 조합하중에 대한 금속 플레이트 接합부의 性能을 평가하기 위한 標準試驗法으로 적용될 수 있을 것이며, 非線形 解析方法은 組合荷重 및 모멘트 性能을 豫測하는데 活用될 수 있다.

Keywords: Nonlinear model, metal plate connection, semi-rigid, interactive load capacity, moment capacity

1. INTRODUCTION

Researches on the connections focused on performance under axial load over the past 25

years. However, studies on modeling of trussed roof assemblies have placed greater emphasis on the importance of connection performance and the need for models to detect their limit state

*1 접수 1994년 10월 5일 Received October 5, 1994

*2 임업연구원 Forestry Research Institute, Seoul 130-012, Korea

*3 서울대학교 농업생명과학대학 College of Agriculture and Life Science, Seoul National University, Suwon 441-744, Korea

load conditions. Recent studies^{1,4)} reported that bending moments had a significant effect on the axial load capacity of the connections in trusses and truss assemblies. Emphasis on the importance of characterizing the strength of the connections under combined axial and transverse load is being increased to achieve more advanced design of wood trusses.

A few researches evaluated moment capacity of the connections and showed limited success at modeling the moment rotation curves up to the point of plate buckling or gap closure. Noguch³⁾ investigated maximum bending moments in pure bending of butt joints with plate connectors theoretically and experimentally. Soltis⁷⁾ analyzed the center support of a two-span beam with truss plates. Hirai²⁾ presented an analytical method for the deformation of wooden beams and frames with semi-rigid joints. Nonlinear analysis method was developed using the principle of virtual work and a stepwise linear approximation.

However, there are no test standards including test apparatus for evaluating joint performance under combined load. Limited knowledge are available to explain analytical procedure for joint performance under combined load. The interaction equation presented by Zahn¹⁰⁾ to characterize wood member load capacity under combined load provides a model that is easily used to define a failure limit state. Wolfe, Hall and Lyles⁹⁾ developed a simple method and apparatus for evaluating the load capacity under combined load and evaluated the load capacity of the connections under axial load and pure bending load. They showed that the axial capacity of the connections decreased significantly when a bending moment is applied in conjunction with axial tension. This kind of analytical model described by Wolfe, Hall, and Lyles⁹⁾ is limited to the elastic analysis with out considering semi-rigid wood joint behavior under combined load.

The objective of this study was to evaluate interactive load and moment capacity for 20

gage galvanized steel plate connections in Korean red pine lumber. An improved eccentric loading apparatus was developed by authors, and joint moment capacity in pure bending was evaluated. Nonlinear analytical models including semi-rigid joint properties were developed to characterize the performance of the connections under combined load.

2. MATERIALS & METHODS

2.1 Material preparation and joint fabrication

Lumber for this study was selected from 38 × 89mm (nominal 2 × 4 inch) lumber of Korean red pine (*Pinus densiflora*) as described in previous paper⁴⁾.

The modulus of elasticity of lumber used for test joints ranged from 75 to 118 × 10³ kgf/cm², with an average of 102 × 10³ kgf/cm². Specific gravity based on oven-dry volume of Korean red pine lumber ranged from 0.45 to 0.59 with an average of 0.53.

Metal plate connectors applied for joints were 20 gage (nominal thickness: 0.89mm) galvanized steel plates manufactured by Truswal Systems Corporation. Connectors for joints were 81.0mm wide by 134.0mm long, and had the same characteristics as the connectors used in previous paper⁴⁾. In all cases, and pure bending, there were 40 teeth per target plate wood interface. Five joints were fabricated for test of each combined loading level. Three groups of joint having different gap were fabricated for pure bending test of galvanized steel plates for the purpose of analyzing the gap effect arising during fabrication; that is, the joints were fabricated to have 0, 1, and 2mm gap between member end. After fabrication, the joint specimens were stored in a conditioning room of 12 percent MC for more than 14 days before testing.

2.2 Test procedure for combined load and pure bending

Eccentric axial tension tests were conducted to evaluate moment capacity and to determine

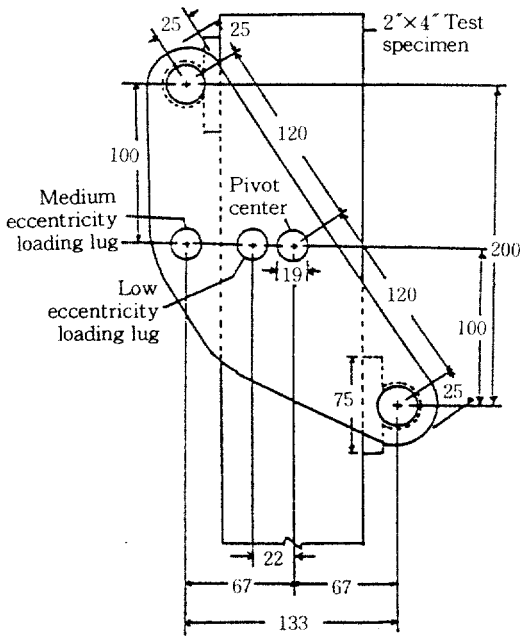


Fig. 1. Eccentric loading apparatus improved by authors(unit: mm).

joint behavior under combined load. Load for joint tests was applied at a constant strain rate of 1.0mm/min using a universal testing machine of 15,000 kgf capacity with and improved eccentric loading apparatus(Fig. 1 and Fig. 2). Two levels of eccentricities were applied by the distance from the pivot center to the loading lug center: 22 and 67mm. Loading apparatus was improved to reduce rotation by moving loading lug up to the same level of the pivot point compared to the apparatus developed by Wolfe⁸⁾.

Pure bending tests with a 100cm span were carried out to evaluate moment capacity of the connections by giving a constant moment section of 60cm length by four point loading.

2.3. Analysis procedure

To describe the characteristics of the connections under combined load using eccentric loading apparatus, it was assumed similar to the report of Wolfe, Hall, and Lyles⁹⁾ that the com-

$$\left(\frac{P}{P_{\max}} \right)^{\alpha} + \left(\frac{M}{M_{\max}} \right)^{\beta} \leq 1 \quad (1)$$

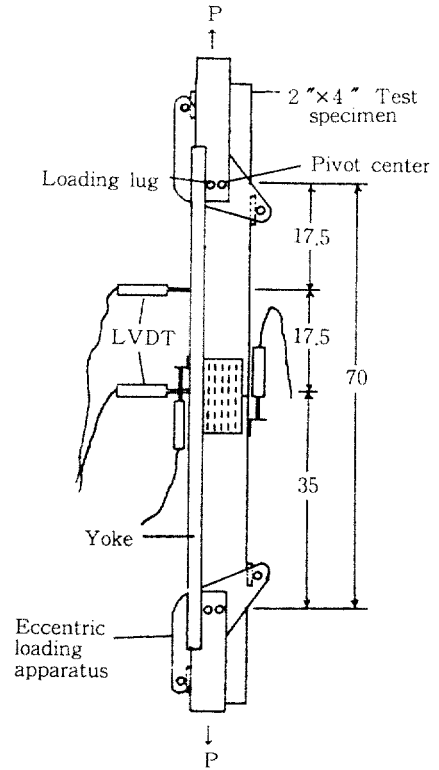


Fig. 2. Joint test arrangement under combined load by improved eccentric loading apparatus by authors (unit: cm).

bination of the load and moment at failure was defined by

where,

P_{\max} : pure axial strength of joint,

M_{\max} : pure bending moment capacity of joint,

P : eccentric axial load at joint,

M : moment at joint, and

α, β : constants assumed to be 1.0 for preliminary analysis.

An analytical model introduced from the elastic curve equation expressed as following

$$\epsilon \left[\frac{\exp(\lambda X) - 1}{\exp(\lambda X) - \exp(-\lambda X)} \exp(-\lambda X) + \frac{1 - \exp(-\lambda X)}{\exp(\lambda X) - \exp(-\lambda X)} \exp(\lambda X) - 1 \right] \quad (2)$$

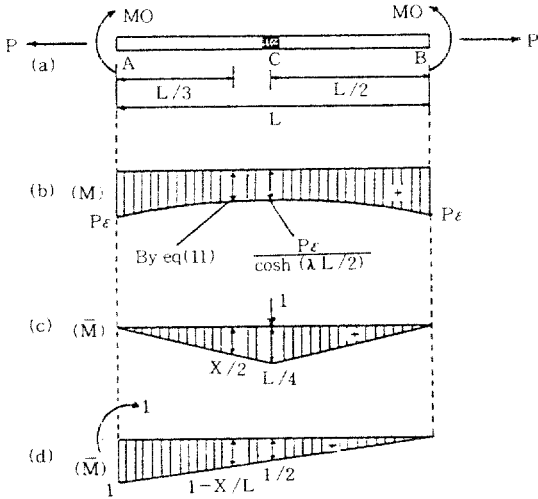


Fig. 3. Structural member with semi-rigid joint under combined load.

where,

Y : beam deflection, and

λ : $\sqrt{P/EI}$

Structural member with semi-rigid joints under combined load was assumed as Fig. 3. The relationship between M_j and θ was derived by the equation, $M_j = \theta R_j$, similar to equation by Hirai²⁾, where, the joint rotational rigidity, R_j , and the rotational angle by moment, θ . By the method of virtual work, the midspan deflection, $Y_{L/2}$, of member that the semi-rigid joint was located, was obtained from the moment diagram presented as \bar{M} and \tilde{M} in Fig. 3.

$$Y_{L/2} = \int_0^L \frac{\bar{M}_x M_x}{EI} dX + \frac{\bar{M}_j M_j}{R_j} \quad (3)$$

where,

M_x : moment along X-axis,

M_j : moment at joint,

\bar{M}_x : moment developed by unit load at the point desired to be calculated, and

\bar{M}_j : moment of joint developed by unit load at the point desired to be calculated.

By equation (3), the midspan deflection became

$$Y = \epsilon \left[1 - \frac{1}{\cosh(\lambda \frac{L}{2})} + \frac{LP}{4R_j \cosh(\lambda \frac{L}{2})} \right] \quad (4)$$

Where,

ϵ : eccentricity, and

L : distance between pivot points at the ends of the beam.

From equation (4), moment of then member was obtained as follow

$$EIY''_{L/2} = \frac{\epsilon}{\cosh(\lambda \frac{L}{2})} + \left[1 - \frac{LP}{4R_j} \right] \quad (5)$$

Where,

EI : member stiffness (E :modulus of elasticity, I : moment of inertia),

Y'' : change in slope over a differential length dX .

This equation accounted for secondary moments that reduce moment at the joint as the specimen deflected laterally.

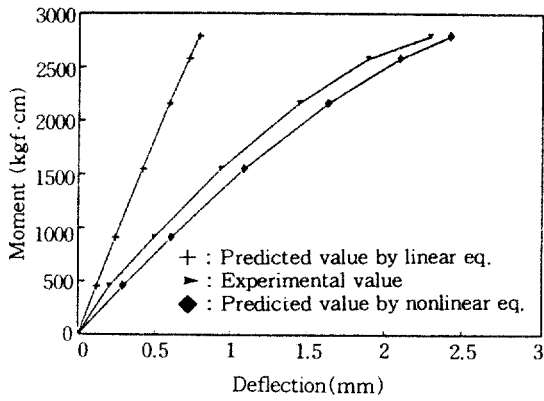
The joint rotational rigidity was obtained from the joint rotational angle. For small displacement, the rotational angle was obtained from the difference of pure bending deflection between members with joint and without joint before cutting. The relationship between the moment and rotational angle was assumed as exponential equation. The nonlinear analysis including semi-rigid properties of the connections was accomplished by these nonlinear analytical processes using the method of virtual work.

3. RESULTS & DISCUSSION

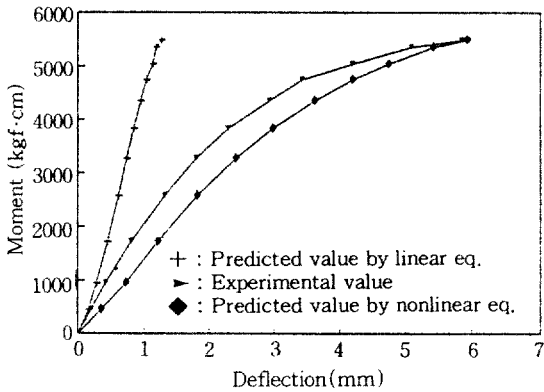
3.1 Interactive load and moment capacity under combined load by linear analytical process

Table 1 and 2 summarize ultimate axial tension load and maximum moments for each group of joint configurations for test joint using two kinds of the connections tested in this study.

Maximum loads in axial tension evaluated



(a) Low eccentricity



(b) Medium eccentricity

Fig. 4. Moment-deflection curves for the connection under combined load.

from the standard joint configuration AA, were used again and averaged 1,908 kgf for the connections as shown in the previous paper⁶⁾. Pure bending moment capacity ranged from 8,850 to 10,060 kgf · cm, and averaged 9,710 kgf · cm for the connections.

The moment at the joint was determined by the combination of the end moment, P_e , derived by load eccentricity, and the secondary moment developed by a secondary effect due to deflection of member. For joint tests in the low eccentricity under combined load, maximum axial loads varied from 1,520 to 1,390 kgf and averaged 1,426 kgf, and maximum moments varied from 3,182 to 2,923 kgf cm and averaged 3,029 kgf · cm. For joint tests in the medium eccentricity under combined load,

Table 1. Ultimate loads for the connections under combined load and pure bending.

Joint configuration	Ultimate axial load		Maximum moment at joint	
	Average CV (kgf)	(%)	Average CV (kgf · cm)	(%)
Combined load				
Low eccentricity	1,426	9.3	3,029	9.3
Medium eccentricity	899	7.4	5,863	7.4
Pure bending				
Without gap	971	7.8	9,710	7.8
With 1mm gap	926	6.4	9,260	6.4
With 2mm gap	863	8.2	8,630	8.2

maximum axial loads varied from 1,004 to 818 kgf and averaged 899 kgf, and maximum moments varied from 6,126 to 5,736 kgf · cm and averaged 5,863 kgf · cm.

For the connections under combined load, axial load ratio (P/P_{max}) for low-and medium-eccentricity averaged 74 and 47 percent, respectively. Moment ratio for low-and medium-eccentricity averaged 31 and 60 percent, respectively. These results were similar to the results by Wolfe⁸⁾. This means that axial capacity was significantly affected by bending moment.

3.2. Nonlinear analysis of interactive moment capacity under combined load

Interactive moment capacity for the connections was calculated from equation (5) including semi-rigid joint properties using nonlinearly varied rotational rigidity. Interactive moment capacity for joint tests in low-and medium-eccentricity averaged 2,792 kgf · cm, and 5,462 kgf · cm, respectively.

Interactive moment capacity for the connections under low-and medium-eccentricity by the model in current study had lower values than those by Wolfe's model by 8.5 and 7.3 percent, respectively. The lower values of moment capacity resulted from this nonlinear process were considered to be due to taking

Table 2. Test results of axial tension, combined axial and bending for the connections.

Target ratio Rp/Rm*1	Axial load capacity			Moment capacity					
	Axial load (kgf)	Axial load CV(%)	Axial ratio**	By Wolfe's model			By authors' model		
				Moment (kgf · cm)	Moment CV(%)	Moment ratio	Moment (kgf · cm)	Moment CV(%)	Moment ratio
1.0/0	1,908	9.7	1	0	0	0	0	0	0
0.5/0.5	1,426	9.3	0.74	3,929	6.7	0.31	2,792	6.6	0.29
0.2/0.8	899	7.4	0.47	5,863	7.4	0.60	5,462	7.4	0.56
0 /1	0	0	0	9,710	7.8	1	9,710	7.8	1

*1 Rp : the ratio of applied axial load to pure axial load capacity Rm : the ratio of applied moment to pure bending capacity.

*2 Axial and moment ratios refer to the ratio of the average axial load and/or bending moment on the joint at the point of failure to strength of samples tested in pure tension and pure bending, respectively.

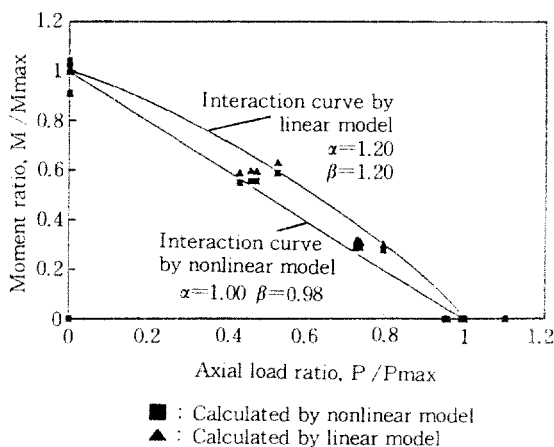


Fig. 5. Combined axial and transverse interaction characteristic curve of the connections.

the effect of secondary moment developed by the rack of rigidity of the connections into account in current study. These were verified by the fact that deflection values calculated by analytical model in current study for the connections under combined load had good agreement with the experimental deflection values (Fig. 4). Moment ratios, which were calculated by the interactive moment capacity for low and medium-eccentricity under combined load, averaged 29 and 56 percent, respectively. Moment ratios by semi-rigid equation (5) including nonlinear analytical

process showed lower values than those by Wolfe's model⁹⁾ by 4 to 2 percent (Table 2).

Interaction curve was derived from axial load ratio and moment ratio as shown in Fig. 5. The results were explained as nonlinear relationships following initial assumption in equation (1). The best curve fitting routine for equation (1) showed values of $\alpha=1.20$ and $\beta=1.20$ in case of using the joint performance calculated by linear model, and $\alpha=1.00$ and $\beta=0.98$ in case of using the joint performance calculated by nonlinear model introduced in this study. These results were similar to the nonlinear relationship resulted by Wolfe⁸⁾. Using these constants, the interactive load and moment capacity under combined load can be estimated from the knowledge of axial capacity by joint tension test and moment capacity by pure bending test.

4. CONCLUSION

This study was accomplished to evaluate interactive load and moment capacity of the connections under combined axial and transverse load using an improved eccentric loading apparatus by authors. Analytical methods were derived to characterize the performance of the semi-rigid joint under combined load by the method of virtual work including nonlinear analysis process.

Interactive moment capacity for the connec-

tions calculated by the model introduced in this study showed more exact values compared to the values calculated by Wolfe's equation, and these were considered to be due to taking into account the effect of secondary moment developed by the rack of rigidity for the connections in this study.

Improved test apparatus by authors deserves consideration for a standard test procedure for evaluating the connections under combined load. The results implicit that nonlinear analysis processes introduced in this study are considered suitable for evaluating interactive load and moment capacity under combined load.

REFERENCES

1. Cramer, S. M., R.W. Wolfe, and A. Peyrot. 1988. Modeling roof systems for reliability analysis. In: Proc. Inter. Conf. on Timber Engineering, Vol. 1., For. Prod. Res. Soc., Madison, Wis.
2. Hirai, T. 1987. Deformation of semi-rigid wooden-frames (1), Beams and frames assembled with nailed gusset plates. Res. Bull. Coll. Exp. For., Hokkaido Univ. 44(1): 279~326
3. Noguchi, M. 1980. Ultimate resisting moment of butt joints with plate connectors stressed in pure bending. *Wood Sci.* 12(3): 168~175
4. Poutanen, T. 1987. Some notes about testing nail plates subjected to moment load. OIB-WIB-Timber Ser. Duboin, Ireland, Sept.
5. Park, M. J., and H. S. Jung. 1994. Analysis of load-displacement characteristics and interactive load capacity model for metal plate connections in wood. Ph. D. Thesis, Seoul National Univ., Seoul
6. Park, M.J. and H.S, Jung. 1994. Analysis of load-displacement characteristics and interactive load capacity model for metal plate connections in wood(I)-load-displacement characteristics. *Mokchae Konghak* 21(4):21~27
7. Soltis, L.A. 1985. Partially continuous floor joists. Res. Pap. FPL 46, USDA For. Ser., For. Prod. Lab., Madison, Wis.
8. Wolfe, R.W. 1990. Metal-plate connections loaded in combined bending and tension. *Forest Prod. J.* 40(9):17~23
9. Wolfe, R.W., M. Hall, and D. Lyles. 1991. Test apparatus for simulating interactive loads on metal wood connections. *J. Testing and Evaluations, JTEVA* 19(6):421~428
10. Zahn, J. 1986. Design of wood members under combined load. *ASCE J. Struct. Eng.* 112(9):2109~2126